

Highly Ionized Sodium X-ray Line Emission from the Solar Corona and the Abundance of Sodium

K. J. H. Phillips¹, K. M. Aggarwal², E. Landi³, and F. P. Keenan²

¹ UCL–Mullard Space Science Laboratory, Holmbury St Mary, Dorking, Surrey RH5 6NT, United Kingdom
e-mail: kjhp@mssl.ucl.ac.uk

² Astrophysics Research Centre, School of Mathematics and Physics, Queen’s University Belfast, Belfast BT7 1NN, N. Ireland, United Kingdom

e-mail: K.Aggarwal@qub.ac.uk, F.Keenan@qub.ac.uk

³ Naval Research Laboratory, Washington, D.C. 20375-5320, U.S.A.

e-mail: enrico.landi@nrl.navy.mil

Received / Accepted

ABSTRACT

Context. The Na x X-ray lines between 10.9 and 11.2 Å have attracted little attention but are of interest since they enable an estimate of the coronal abundance of Na to be made. This is of great interest in the continuing debate on the nature of the FIP (first ionization potential) effect.

Aims. Observations of the Na x lines with the Solar Maximum Mission Flat Crystal Spectrometer and a rocket-borne X-ray spectrometer are used to measure the Na/Ne abundance ratio, i.e. the ratio of an element with very low FIP to one with high FIP.

Methods. New atomic data are used to generate synthetic spectra which are compared with the observations, with temperature and the Na/Ne abundance ratio as free parameters.

Results. Temperature estimates from the observations indicate that the line emission is principally from non-flaring active regions, and that the Na/Ne abundance ratio is $0.07 \pm 50\%$.

Conclusions. The Na/Ne abundance ratio is close to a coronal value for which the abundances of low-FIP elements (FIP < 10 eV) are enhanced by a factor of 3 to 4 over those found in the photosphere. For low-temperature ($T_e \leq 1.5$ MK) spectra, the presence of Fe xvii lines requires that either a higher-temperature component is present or a revision of ionization or recombination rates is needed.

Key words. Line: identification—Sun: abundances—Sun: corona—Sun: flares—Sun: X-rays, gamma rays

1. Introduction

Sodium has few prominent or unblended emission lines in the ultraviolet and X-ray spectra emitted by solar coronal plasmas. Hence determinations of its abundance relative to other elements rely on measurements of emission line fluxes that are either weak or in crowded spectral regions. Yet its abundance is important for discussions of the so-called FIP effect, whereby coronal element abundances differ from corresponding photospheric values depending on whether their first ionization potential (FIP) is greater or less than about 10 eV (Meyer, 1985; Feldman et al., 1992a). This is because the FIP of Na is only 5.14 eV, less than any other element common in the Sun apart from potassium, which has an FIP of 4.34 eV. Determinations of the coronal abundance of either Na or K can therefore probe the possibility that elements with small FIP are enhanced by amounts that depend on the magnitude of the FIP, as is suggested by the electric current model of Hénoux & Somov (1997) to explain the FIP effect. Observational evidence for this has been provided by Feldman (1993), and to some extent by observations of He-like K X-ray lines seen in numerous flares and non-flare periods between 2002 and 2005 with the RESIK spectrometer (Sylwester et al., 2010). Coronal sodium emission lines include the Li-like Na (Na ix) resonance lines $1s^2 2s^2 S_{1/2} - 1s^2 2p^2 P_{1/2}$,

$^2P_{3/2}$ in the extreme ultraviolet, at 681.7 Å and 694.3 Å, and the He-like Na (Na x) line $1s2s^3S_1 - 1s2p^3P_2$ at 1111.76 Å seen in *SOHO* SUMER spectra (Curdt et al., 2000, 2001), and resonance lines of H-like (Na xi) and He-like Na (Na x) in the soft X-ray range. X-ray observations of the Na x and Na xi X-ray emission lines should in principle be easier than for the equivalent potassium lines as the photospheric abundance of Na is higher by a factor of 16 than K (Asplund et al., 2009), but nevertheless observations remain scarce. The Na xi Ly- α and Ly- β lines are at 10.02 Å and 8.46 Å respectively, and the Na x $1s^2 - 1s2l$ ($l = s, p$) lines are near 11 Å. The Ly- β line was observed by Walker et al. (1974) with crystal spectrometers on the *OVI-17* spacecraft, and the Na x lines with rocket-borne crystal spectrometers by Parkinson (1975). Only a single scan of the Flat Crystal Spectrometer (FCS) on *Solar Maximum Mission* (SMM) in its 9-year lifetime was made of the Na x lines during a flare in 1980 (Phillips et al., 1982). Previous Na abundance analyses of the *OVI-17* data gave $\log A(\text{Na}) = 6.26$ (Walker et al., 1974) and of the Parkinson rocket data $\log A(\text{Na}) = 6.73$ (Parkinson, 1975) (on a scale $\log A(\text{H}) = 12$). The Na x and Na xi X-ray lines have incidentally been observed in radiation from a laboratory (Z-pinch) device by Burkhalter et al. (1990).

Only rather approximate atomic data were available at the time of the Walker et al. (1974) and Parkinson (1975) analyses. However, significant advances have since been made to evaluate collisional excitation rate coefficients and ionization fractions

Send offprint requests to: K. J. H. Phillips e-mail: kjhp@mssl.ucl.ac.uk

needed for the evaluation of the abundance of sodium from X-ray line fluxes. The CHIANTI database and software package in the Interactive Data Language (IDL) SolarSoftWare system, since its inception in the late 1990s (Dere et al., 1997, 2009), has also simplified analyses of X-ray and ultraviolet spectral data considerably. Excitation data for the Na x lines presently included in CHIANTI are interpolated values from other elements, but more recently Aggarwal et al. (2009) have calculated collisional excitation data specifically for He-like sodium with the close-coupling *R*-matrix code. Also, more refined ionization fractions assuming coronal ionization equilibrium have recently been calculated by Bryans et al. (2009).

The availability of new atomic data has inspired a fresh analysis, reported here, of the Na x X-ray lines seen in the *SMM* FCS spectral scan and the spectra obtained by Parkinson (1975). X-ray lines of Na x were identified by Phillips et al. (1982), with more detailed analysis of nearby lines by Landi & Phillips (2005). A slight revision of spectral line identifications is given here and a determination of the Na/Ne abundance ratio for this flare plasma, based on a remarkable coincidence of the contribution functions of the Na x *w* line and that of the Ne ix $1s^2 - 1s4p$ (*w4* or He- γ) line blended with the Na x *w* line. The Na/Ne abundance ratio is examined in the light of other recent abundance determinations and the nature of the FIP effect in solar coronal plasmas.

2. Observations

The *SMM* FCS observations (Phillips et al., 1982) were made during the decay stage of a *GOES* M1.5 class flare on 1980 August 25 with channel 2 of seven channels making up the instrument. Scanning flat crystals were mounted on a rotatable shaft, and radiation incident on them was via a grid collimator giving a 14 arcsecond (FWHM) field-of-view. The high-precision Baldwin drive–encoder units used to rotate the drive led to very accurate wavelengths for observed spectral lines. The whole FCS could also be scanned spatially across an emitting region on the Sun. For the 1980 flare, a spatial scan was made over the flare emission near its onset to determine the location of the brightest point. The instrument was then pointed to this position, and a complete spectral scan taken. High-quality beryl ($\text{Be}_3\text{Al}_2\text{Si}_6\text{O}_{18}$, $2d = 15.96 \text{ \AA}$) was the diffracting crystal of channel 2, giving a spectral resolution of 0.0056 \AA at the wavelengths of the Na x lines near 11 \AA . The scan took 17 minutes to accomplish, during which time there was a significant change in the emitting region. An analysis of the FCS data in this flare with CHIANTI (Landi & Phillips, 2005) took this into account, dividing the scan into seven time bins. The Na x lines near 11 \AA lay at the end of time bin 1 and the start of time bin 2 of the scan, when the flare emission and temperature were still high. An emission measure analysis by Landi & Phillips (2005) using only Fe lines (stages Fe xvii to Fe xxiii) indicated a temperature of about 8 MK, which is reasonable for a M1.5 class flare a few minutes after its maximum emission. This analysis omitted emission lines of He-like ions such as Ne ix and Mg xi since they indicated a much lower temperature, of about 1–4 MK. The reason for this is that the emission measure appears to have a bimodal distribution, with a flare component ($\sim 8 \text{ MK}$) and a lower-temperature component attributable to the non-flaring host active region which gives rise to the emission from the He-like ions. The Na x emission lines appear to be in the latter category. Support for such emission measure distributions is provided by analysis of Ar xvii X-ray lines observed during flares

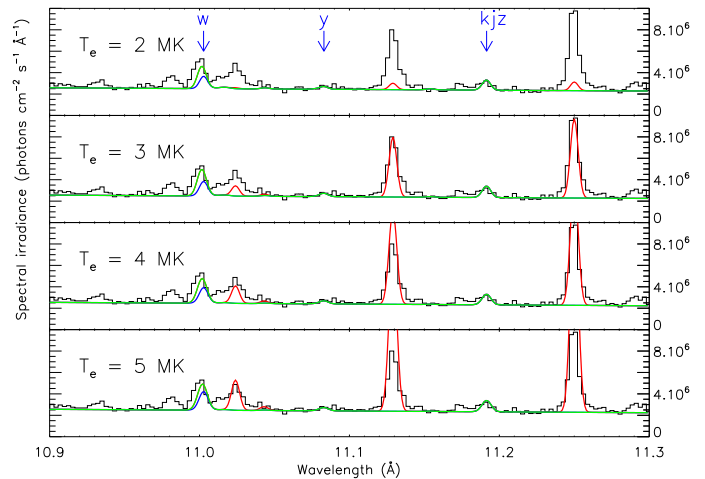


Fig. 1. X-ray spectrum in the 10.9–11.3 Å range obtained with the *SMM* FCS during the decay of the 1980 August 25 flare (histogram) with theoretical spectra for temperatures 2 MK, 3MK, 4 MK, and 5 MK (indicated in each panel) and an assumed Ne/Na abundance ratio equal to the coronal value of 0.07 (Feldman et al., 1992a). Line styles for the theoretical curves: continuous line = Na x lines alone (including weak Na ix satellites); dot-dash line = Na x and Ne ix lines; dotted line = with Fe xvii lines. The positions of the principal Na x lines *w*, *y*, and *z* are indicated (the Na ix satellites *j* and *k* are within 0.004 \AA of line *z*), and the Ne ix *w4* line is at 11.000 \AA . The other prominent lines are due to Fe xvii, with observed wavelengths 11.023 \AA , 11.133 \AA , and 11.253 \AA (see Table 1). (A colour version is available in the on-line journal. On-line journal version key: black histogram = observed spectrum; coloured curves are theoretical spectra, with code blue = Na x lines alone; green = Na x and Ne ix lines; red = with Fe xvii lines.)

by the RESIK instrument (Sylwester et al., 2008); in that case, Ar xvii line ratios were best fitted by a bimodal emission measure distribution having temperatures of 4.5 MK and 16 MK. Also, analysis of broad-band data from the *RHESSI* instrument in its A0 attenuator state (Phillips et al., 2006) similarly indicates that there is a non-flaring component of emission, with temperature corresponding to the active region, as well as a hotter flare component.

The FCS channel 2 spectral scan over the 10.9–11.3 Å range is shown in each of the four panels of Figure 1 (histogram plot). In these plots, FCS count rates have been converted to absolute spectral irradiance units using pre-launch intensity calibration factors. The background emission is largely due to fluorescence of the crystal material with the solar continuum making a minor contribution. The theoretical wavelengths of Na x lines are indicated.

The rocket-borne crystal spectrometers described by Parkinson (1975) were launched on a stabilised Skylark rocket on 1971 November 30. The instruments viewed a non-flaring active region on the Sun through a multi-grid collimator with field of view equal to 3 arcminutes (FWHM). Two of the spectrometers scanned through the region of the Na x lines near 11 \AA with KAP ($2d = 26.64 \text{ \AA}$) and gypsum ($2d = 15.19 \text{ \AA}$) crystal. As the data are no longer in digital form, the spectra in the region of the Na x lines (10.9–11.4 Å) from Figure 3 of Parkinson (1975) were hand-digitised for the purposes of this analysis. The photon count rate is higher in the KAP crystal scan and so the spectrum

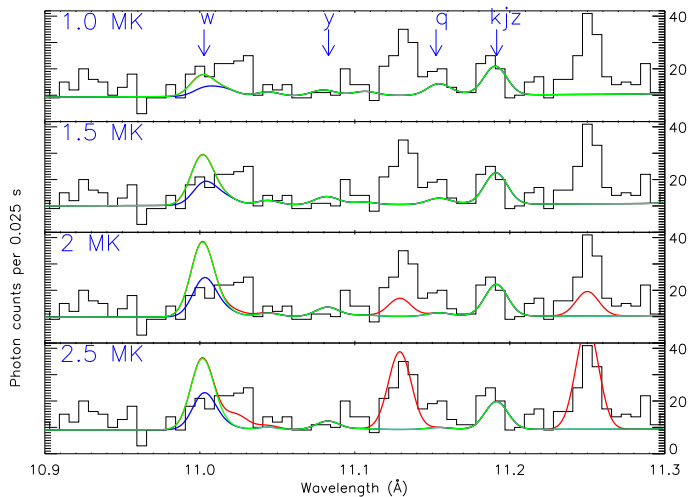


Fig. 2. X-ray spectrum (histograms) in the 10.9–11.3 Å range obtained with a rocket-borne KAP crystal spectrometer of a non-flaring active region in 1971 (Parkinson, 1975). The spectrum is compared with synthetic spectra having temperatures 1 MK, 1.5 MK, 2 MK, and 2.5 MK (indicated in each panel) and an assumed Ne/Na abundance ratio equal to a coronal value of 0.07. Na ix satellites are included in the synthetic spectra. Line styles are as for Figure 1. (A colour version is available in the on-line journal. On-line journal version key: black histogram = observed spectrum; coloured curves are theoretical spectra, with code blue = Na x lines alone; green = Na x and Ne ix lines; red = with Fe xvii lines.)

has high statistical quality. This scan is shown in Figure 2. The temperature is likely to be lower than the FCS scan in Figure 1 and the line feature at 11.152 Å, if real, could be the Na ix satellites *q* and *r*; the theoretical position of line *q* is indicated.

3. Atomic data and line identifications

3.1. The spectrum in the 10.9–11.3 Å region

Na x lines in the X-ray region include a group of four lines with transitions of the type $1s^2 - 1s2l$ ($l = s, p$) and higher members of the $1s^2 - 1snl$ series. Using the notation of Gabriel (1972), the $n = 2$ lines are, in increasing order of wavelength, identified with letters *w* (transition $1s^2 \ ^1S_0 - 1s2p \ ^1P_1$, wavelength 11.003 Å), *x* ($1s^2 \ ^1S_0 - 1s2p \ ^3P_1$, 11.080 Å), *y* ($1s^2 \ ^1S_0 - 1s2p \ ^3P_2$, 11.083 Å), and *z* ($1s^2 \ ^1S_0 - 1s2s \ ^3S_1$, 11.192 Å). The wavelengths, quoted from CHIANTI, are from Ralchenko et al. (2008). Dielectronic satellites with transitions $1s^2 n' l' - 1s2pn' l'$ occur in great profusion in the neighbourhood of the *w*-*z* lines, but with only a few that are significant at lower temperatures, particularly satellites *j* and *k* (transitions $1s^2 2p - 1s2p^2$) which blend with line *z* and satellites *q* and *r* ($1s^2 2s - 1s2s2p$). Numerous satellites with very high *n* values occur near line *w* and converge on it; individually they are not important but their cumulative contribution is up to about 10% of line *w*.

The Ne ix $1s^2 \ ^1S_0 - 1s4p \ ^1P_1$ (*w4*) line occurs very near the Na x *w* line, but how near was unclear from early atomic structure calculations. Those of Vainshtein & Safronova (1978) gave the wavelength as 11.025 Å, longward of the Na x *w* line by an amount easily resolvable with the FCS and Parkinson instruments. Using the wavelengths of Wiese et al. (1969), Parkinson (1975) was led to identify a line feature at 11.027 Å as the

Ne ix *w4* line. However, the more recent MCDF calculations of Chen et al. (2006) seem to have established that this line is at 11.000 Å, just 0.003 Å away from the Na x *w* line. In light of this, the feature at 11.027 Å is now identifiable with an Fe xvii line with transition $2s^2 \ 2p^6 \ ^1S_0 - 2s \ 2p^6 \ 4p \ ^1P_1$ (wavelength 11.023 Å according to Landi & Phillips (2005)). More intense Fe xvii lines occur at 11.133 Å and 11.253 Å. Table 1 lists identifications and wavelengths of the principal lines in this region.

Ne viii satellite lines with transitions $1s^2 \ nl - 1s \ nl \ 4p$ are expected to form weak features to the long-wavelength side of the Ne ix *w4* line, but are outside the range of interest here: the most prominent are those in the $1s^2 \ 2p - 1s \ 2p \ 4p$ array which are located at ~ 11.45 Å.

3.2. Contribution functions

The contribution function $G(T_e)$, defining the temperature range of significant emission of a line emitted by an ion (stage $+m$) of element X in a transition from an excited level *j* to the ground level, is defined by (e.g. Phillips et al. (2008))

$$G(T_e) = \frac{N(X_j^{+m}) N(X^{+m}) N(X) N(H)}{N(X^{+m}) N(X) N(H) N_e} N_e \quad (1)$$

where the number densities N are of the excited level of ion X_j^{+m} , the ion X^{+m} (all levels summed), the element X (all ionization stages *m*), and hydrogen (H), and N_e is the electron density. The abundance of X relative to H is $N(X)/N(H) = A(X)$, and for a coronal plasma $N(H)/N_e$ is 0.8. These functions can be determined from CHIANTI with the user supplying the line wavelength and a chosen set of ionization fractions and element abundances. Figure 3 shows the CHIANTI $G(T_e)$ functions for the lines of interest here, viz. Na x *w*, Ne ix *w4*, and the Fe xvii line at 11.129 Å. The excitation data for the Na x lines used in these calculations are from interpolation of distorted-wave calculations for neighbouring ions, while those for the Ne ix lines are from the *R*-matrix calculations of Chen et al. (2006). The recent ionization fractions of Bryans et al. (2009) were used, as were the coronal abundances of Feldman et al. (1992a), in which low-FIP elements have abundances enhanced over photospheric values by a factor of ~ 4 but high-FIP element abundances are equal to photospheric values (see §3.5).

While the Fe xvii $G(T_e)$ curve steeply rises at $T_e \lesssim 4$ MK and falls at $T_e \gtrsim 10$ MK, reflecting the fractional abundance of the Fe⁺¹⁶ ion, both the Na x and Ne ix lines have contribution functions that are much more slowly decreasing with T_e . There is a remarkable coincidence of the Na x and Ne ix curves for $T_e \lesssim 4$ MK, and even at higher temperatures the Na x curve is consistently only a factor 3 above the Ne ix curve. This provides a means for determining the Na/Ne abundance if the two lines, which are practically unresolvable with the FCS and Parkinson spectrometers, are mostly emitted at temperatures $\lesssim 4$ MK.

3.3. Theoretical Na X line fluxes

The principal Na x X-ray lines in the 10.9–11.3 Å range are mostly excited by electron collisions, and so collisional excitation rate coefficients are of considerable importance in synthesizing the spectra. As mentioned, the CHIANTI data use interpolated distorted-wave calculations, but recent excitation data of Aggarwal et al. (2009) using the close-coupling *R*-matrix code developed at Queen's University Belfast should be a significant improvement and were used here. The data are in the form of

Table 1. Principal lines in the 10.9–11.3 Å region.

Wavelength (Å) ^(a)	Ion	Line label	Transition
11.000	Ne IX	w4	$1s^2\ ^1S_0 - 1s4p\ ^1P_1$
11.003	Na X	w	$1s^2\ ^1S_0 - 1s2p\ ^1P_1$
11.023	Fe XVII		$2s^2\ 2p^6\ ^1S_0 - 2s2p^6\ 4p\ ^1P_1$
11.080	Na X	x	$1s^2\ ^1S_0 - 1s2p\ ^3P_2$
11.083	Na X	y	$1s^2\ ^1S_0 - 1s2p\ ^3P_1$
11.133	Fe XVII		$2s^2\ 2p^6\ ^1S_0 - 2s^2\ 2p^5\ 5d\ ^1P_1$
11.192	Na X	z	$1s^2\ ^1S_0 - 1s2s\ ^3S_1$
11.253	Fe XVII		$2s^2\ 2p^6\ ^1S_0 - 2s^2\ 2p^5\ 5d\ ^3D_1$

Note: (a) Wavelengths from Landi & Phillips (2005).

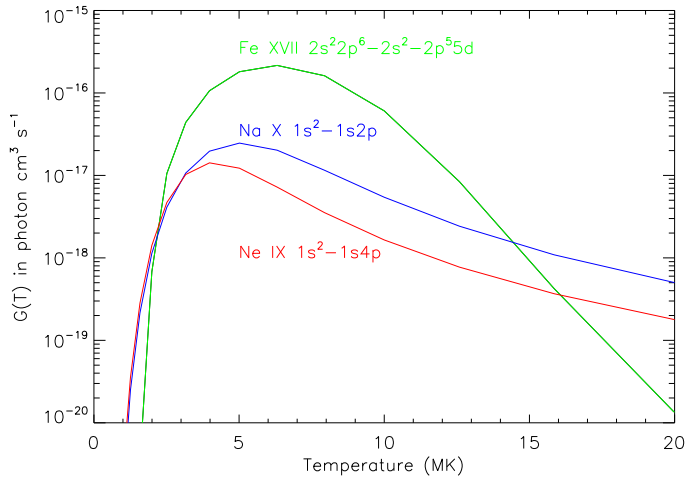


Fig. 3. Contribution functions $G(T_e)$ for lines in the 10.9–11.2 Å range: Na x w $1s^2\ ^1S_0 - 1s2p\ ^1P_1$ 11.003 Å; Ne ix w4 $1s^2\ ^1S_0 - 1s4p\ ^1P_1$ 11.000 Å; Fe xvii $2s^2\ 2p^6\ ^1S_0 - 2s^2\ 2p^5\ 5d\ ^1P_1$ 11.129 Å. The contribution functions of the Na x and Ne ix lines are almost identical for $T_e < 3$ MK. (A colour version is available in the on-line journal. On-line journal version key: blue curve = Na x w line; red = Ne ix w4 line; green = Fe xvii 11.129 Å line.)

temperature-averaged collision strengths $\Upsilon(T_e)$ for the various transitions involved, and include auto-ionizing resonances which make a contribution to the Υ s if near the excitation threshold. For the Na x w line, the excitation is mostly from the ground state $1s^2\ ^1S_0$ to the upper level $1s2p\ ^1P_1$, with spontaneous radiative transition from the upper level. However, for the x, y, and z lines in which the upper levels are triplets ($1s2s\ ^3S_1$ or $1s2p\ ^3P$), other transitions are involved. Cascade transitions from higher levels $1s\ n\ l$ where $n > 3$ are important, especially for lines x, y, and z, as are transitions from the upper levels of each line resulting from recombination of the H-like stage of Na (Na^{+10}). The new excitation data were entered into CHIANTI data files so that Na x line fluxes could be obtained. While the differences in the x, y, and z line fluxes between the original interpolated data from CHIANTI and the new R -matrix results are rather modest ($\leq 7\%$), they are up to 22% ($T_e = 3$ MK) for the important w line.

3.4. Na IX dielectronic satellites

Dielectronic satellite line emission is an important contributor to X-ray spectra of He-like and H-like ions, particularly those with high atomic number Z . The CHIANTI database currently has no dielectronic satellite excitation data for satellites due to Li-like Na which occur near the Na x X-ray lines, having transitions

$1s^2\ n\ l - 1s2p\ n\ l$ ($n\ l$ being the quantum numbers of the “spectator” electron in the transition: see Gabriel (1972)). Previous calculations have used a variety of atomic codes to obtain these data; here we used an adaptation of the Cowan pseudo-relativistic Hartree-Fock (HFR) code (Cowan, 1981) for small personal computers designed by A. Kramida (2008, priv. comm.).

The data concerned are the satellite (sat) wavelength and an intensity factor B_{sat} . A satellite line is excited by dielectronic recombination when an electron recombines with a He-like Na ion (Na^{+9}) to produce a doubly excited state which then radiatively de-excites. The flux at the Earth (distance from Sun = 1 AU) of the satellite F_{diel} formed in this way is given by

$$F_{\text{diel}} = 2.07 \times 10^{-16} \frac{N(\text{Na}^{+9})N_e V}{4\pi(\text{AU})^2} \frac{A_r A_a}{A_a + \Sigma A_r} \frac{\exp(-E_{\text{sat}}/k_B T_e)}{T_e^{3/2}} \quad (2)$$

where A_r and A_a are the radiative and autoionization probabilities from the satellite’s upper level respectively, E_{sat} the energy of the upper level with respect to the ground level of the Na^{+9} ion, V the flare emitting volume, and k_B is Boltzmann’s constant. The term $N(\text{Na}^{+9})N_e V$ can be rewritten $0.8f(\text{Na}^{+9})A(\text{Na})EM$ where the volume emission measure is $EM = N_e^2 V$ and the fraction of Na^{+9} ions, $N(\text{Na}^{+9})/\Sigma N(\text{Na}^{+m})$, is $f(T_e)$. The intensity factor B_{sat} , defined by

$$B_{\text{sat}} = \frac{A_r A_a}{A_a + \Sigma A_r}, \quad (3)$$

is calculated by the Cowan HFR code together with all the radiative and autoionization probabilities and the satellite wavelengths.

Input to the code is the satellite array and value of E_{sat} . Single-electron radial functions are calculated by the code and combined with Slater–Condon theory to give energy levels. Previous experience (Phillips et al., 1994) has shown that choosing 100% for the scaling of the Slater parameters in the code gives good results for X-ray transitions, though there is generally a small wavelength shift $\Delta\lambda$ between the wavelength of the He-like ion line w and that of satellites with very high values of n for the spectator electron, which should converge on line w. In running the code for Na ix satellites, we took 100% scaling of the Slater parameters and added $\Delta\lambda = +0.001$ Å to the Cowan satellite wavelengths since this value of $\Delta\lambda$ is needed to achieve agreement between the wavelengths of high- n satellites and the Na x w line.

Table 2 lists data for a selection of satellites – wavelengths, B_{sat} , and E_{sat} – from the calculations, which included satellites with spectator electrons having $n\ l = 2s, 2p, 3s, 3p, 3d$, etc., extending up to $n\ l = 6p$. We generated data for $n\ l = 10p$ to determine the wavelength shift $\Delta\lambda$. As was found by Gabriel (1972) and others, satellites j and k (see Table 2) are the most intense,

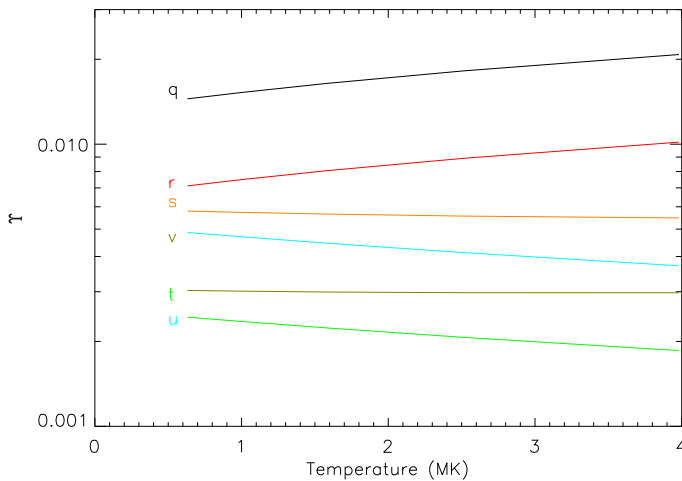


Fig. 4. Maxwellian-averaged collision strengths $\Upsilon(T_e)$ as a function of temperature for excitation from the Li-like Na (Na^{+8}) ion ground level $1s^2 2s^2 S_{1/2}$ to the upper levels of satellites q , r , s , t , u , and v (transitions given in Table 2) calculated using the Flexible Atomic Code (FAC). (A colour version is available in the on-line journal, with different colours for the Υ curves for excitation to each upper level.)

i.e. have the largest values of B_{sat} . They are both within 0.004 \AA of the $\text{Na } x \text{ z}$ line at 11.192 \AA . This is in agreement with other calculations of satellite line wavelengths for elements having similar atomic number, notably Mg (e.g. Steenman-Clark et al. (1984)). For Ca ($Z = 20$), satellite k becomes resolved from line z , while for Fe ($Z = 26$), both j and k are resolved.

Inner-shell excitation can also give rise to satellites in the $1s^2 2s - 1s 2s 2p$ array for solar flare densities (at much higher densities, inner-shell excitation gives rise to satellites in other arrays also). Again, the current version of CHIANTI does not have atomic data relating to these satellites. As at least satellites q and r (see Table 2) in the $1s^2 2s - 1s 2s 2p$ array are expected to be important, Maxwellian-averaged collision strengths $\Upsilon(T_e)$ for the entire array were calculated using the Flexible Atomic Code of Gu (2003). Assuming that the de-excitation is entirely the radiative transition to the ground level $1s^2 2s^2 S_{1/2}$, the satellite line fluxes are then given by

$$F_{i-s} = \frac{N(\text{Na}^{+8})N_e V}{4\pi(\text{AU})^2} \times \frac{8.63 \times 10^{-6} \Upsilon(T_e)}{T_e^{1/2}} \exp(-E_{\text{exc}}/k_B T_e) \quad (4)$$

where E_{exc} is the excitation energy of the satellite line. Figure 4 shows the calculated Υ functions for excitation from the $1s^2 2s^2 S_{1/2}$ level to the levels indicated.

3.5. Synthetic spectra

A spectral synthesis program was written with the specific intention of matching the $\text{Na } x$ and $\text{Ne } ix$ lines, together with $\text{Na } ix$ satellites, in the $10.9\text{--}11.3 \text{ \AA}$ region as observed by the FCS and Parkinson spectrometer. It is assumed, as was found from the RESIK flare observations of $\text{Ar } xvii$ line ratios (Sylwester et al., 2008) and analysis of broad-band spectra from *RHESSI* in its A0 attenuator state (Phillips et al., 2006), that a two-component emission measure distribution describes the observed spectra, a low-temperature component (1–4 MK) appropriate for the $\text{Na } x$ and $\text{Ne } ix$ emission from the non-flaring active region and a higher-temperature component for the flare emission proper

(FCS spectrum) or for a hotter part of the active region if present (Parkinson spectra): it is this component that is responsible for most of the Fe ion line emission in this region, including $\text{Fe } xix$ and $\text{Fe } xxiii$ lines seen in the FCS spectrum and which were fitted by an 8 MK component in the analysis by Landi & Phillips (2005). The $\text{Fe } xvii$ lines are emitted by plasma with $T_e > 3 \text{ MK}$ (see Figure 3) so contributions from both the active region and flare may be expected. The synthesis program computed spectra in a temperature grid from 0.8 MK to 5 MK.

The $\text{Na } x$ lines were included in the synthesis program from the Aggarwal et al. (2009) atomic data (§3.3) and the $\text{Na } ix$ satellites, both those excited by dielectronic recombination and those formed by inner-shell excitation, from the data discussed in §3.4. The $\text{Ne } ix \text{ w}4$ line was included using fluxes from CHIANTI, as well as the much weaker intercombination line $1s^2 \text{ } ^1S_0 - 1s4p \text{ } ^3P_1$, unresolvable from the $\text{w}4$ line. Other lines were also included, most notably $\text{Fe } xvii$ lines; lines of $\text{Fe } xix$ and $\text{Fe } xxiii$ had negligible fluxes in the temperature range considered. The CHIANTI $\text{Fe } xvii$ line wavelengths differ somewhat from the observed FCS wavelengths; as the FCS wavelengths are expected to be very precise (uncertainties $\lesssim 2 \text{ m\AA}$ in this region), the FCS wavelengths from an original analysis (Phillips et al., 1982) were used. Fluxes of the $\text{Na } x \text{ w, x, y, and z}$ lines were obtained from the collisional excitation data of Aggarwal et al. (2009) which were inserted into files that could be read by the CHIANTI software. The $\text{Na } ix$ satellite fluxes were calculated from equations (2) and (4). Gaussian profiles were applied to spectral lines that were a convolution of the thermal Doppler broadening (FWHM width $\Delta\lambda_D$) and the instrumental profile, defined by the crystal rocking curve (FWHM width equal to $\Delta\lambda_{\text{rc}}$), assumed to be Gaussian. The widths are given respectively by

$$\Delta\lambda_D = 1.665 \frac{\lambda}{c} \left(\frac{2k_B T_{\text{ion}}}{M_{\text{ion}}} \right)^{1/2} \quad (5)$$

where T_{ion} is the temperature of the emitting ion, taken to be T_e , and M_{ion} the ion mass, and

$$\Delta\lambda_{\text{rc}} = 2d \cos \theta \Delta\theta \quad (6)$$

where the crystal rocking curve is $\Delta\theta$. A pre-launch measured value of $\Delta\theta$ for the FCS observing the $\text{Na } x$ lines of 100 arcseconds was taken for the FCS spectrum. The differing ion masses for the $\text{Na } x$, $\text{Ne } ix$, and $\text{Fe } xvii$ lines were taken into account, though the FCS instrumental broadening dominates the convolved line profile. For the Parkinson rocket spectra, the instrument profile was empirically taken to be 3 times the FCS rocking curve width to match the observed line profiles. As in the calculation of contribution functions (§3.2), the Na and Ne ionization fractions were taken from Bryans et al. (2009).

Element abundances were taken for an average coronal plasma using values from Feldman et al. (1992a) (included as ‘‘coronal abundances’’ in CHIANTI). An initial value of 0.071 is thus taken for the sodium-to-neon abundance ratio – $A(\text{Na})/A(\text{Ne})$ – but in our analysis it is a free parameter to be determined from line flux measurements. The Fe abundance likewise is taken to be $\log A(\text{Fe}) = 8.10$ (on a scale $\log A(\text{H}) = 12$). This is supported by measurements of broad-band *RHESSI* flare spectra Phillips et al. (2006), indicating that of 27 flares, 19 had estimated abundances $\log A(\text{Fe})$ that were within 20% of the Feldman et al. (1992a) value. Although spatial variations in coronal abundances have been noted (Feldman et al., 1992b), the chief variations are those during impulsive flares and above strong sunspot magnetic fields, when low-FIP elements appear to have photospheric abundances.

Table 2. Selected Na ix satellite lines excited by dielectronic recombination: data from the Cowan HFR code.

Wavelength (Å) ^(a)	Line label ^(b)	Transition	B_{sat} (s ⁻¹) ^(c)	E_{sat} (Ry)
11.043	<i>d15</i>	$1s^2 3p^2 P_{1/2} - 1s 2p 3p ({}^1P)^2 D_{3/2}$	3.33(13)	73.5
11.044	<i>d13</i>	$1s^2 3p^2 P_{3/2} - 1s 2p 3p ({}^1P)^2 D_{5/2}$	5.77(13)	73.5
11.077 ^(d)	<i>s</i>	$1s^2 2s^2 S_{1/2} - 1s 2p^2 ({}^3S)^2 P_{3/2}$	4.64(12)	60.0
11.078 ^(d)	<i>t</i>	$1s^2 2s^2 S_{1/2} - 1s 2s 2p ({}^3S)^2 P_{1/2}$	2.90(12)	60.0
11.105	<i>n</i>	$1s^2 2p^2 P_{1/2} - 1s 2p^2 {}^2S_{1/2}$	3.11(12)	60.6
11.108	<i>m</i>	$1s^2 2p^2 P_{3/2} - 1s 2p^2 {}^2S_{1/2}$	8.19(12)	60.6
11.152 ^(d)	<i>q</i>	$1s^2 2s^2 S_{1/2} - 1s 2s 2p ({}^1S)^2 P_{3/2}$	1.66(13)	60.6
11.155 ^(d)	<i>r</i>	$1s^2 2s^2 S_{1/2} - 1s 2s 2p ({}^1S)^2 P_{1/2}$	9.61(12)	60.6
11.165	<i>b</i>	$1s^2 2p^2 P_{1/2} - 1s 2p^2 {}^2P_{3/2}$	3.28(11)	60.6
11.168	<i>d</i>	$1s^2 2p^2 P_{1/2} - 1s 2p^2 {}^2P_{1/2}$	7.12(10)	60.6
11.168	<i>a</i>	$1s^2 2p^2 P_{3/2} - 1s 2p^2 {}^2P_{3/2}$	2.13(12)	60.6
11.171	<i>c</i>	$1s^2 2p^2 P_{3/2} - 1s 2p^2 {}^2P_{1/2}$	3.25(10)	60.6
11.188	<i>k</i>	$1s^2 2p^2 P_{1/2} - 1s 2p^2 {}^2D_{3/2}$	2.31(13)	60.6
11.191	<i>j</i>	$1s^2 2p^2 P_{3/2} - 1s 2p^2 {}^2D_{5/2}$	3.70(13)	60.6
11.192	<i>l</i>	$1s^2 2p^2 P_{3/2} - 1s 2p^2 {}^2D_{3/2}$	1.90(12)	60.6
11.286	<i>e</i>	$1s^2 2p^2 P_{3/2} - 1s 2p^2 {}^4P_{5/2}$	1.74(10)	60.6
11.298 ^(d)	<i>u</i>	$1s^2 2s^2 S_{1/2} - 1s 2p^2 ({}^3S)^4 P_{3/2}$	3.45(9)	60.0
11.300 ^(d)	<i>v</i>	$1s^2 2s^2 S_{1/2} - 1s 2s 2p ({}^3S)^4 P_{1/2}$	6.64(8)	60.0

Note: (a) Wavelengths from Cowan code + 0.001 Å; (b) Notation of Gabriel (1972); Bely-Dubau et al. (1979); (c) Numbers in parentheses are powers of ten; (d) Lines also formed by inner-shell excitation.

4. Results

Figure 1 shows the *SMM* FCS spectrum for the flare of 1980 August 25. In this figure, the observed spectrum is compared with four synthetic spectra with $T_e = 2, 3, 4, 5$ MK, all with the coronal value of $A(\text{Na})/A(\text{Ne}) = 0.071$. In each case, the synthetic spectra were adjusted so that the blend of the Na x *z* line with the Na ix *j* and *k* satellites (feature at 11.192 Å) is fitted, leaving the blend of the Na ix *w* line and the Ne ix *w4* line (feature at 11.003 Å) free as well as the barely significant Na x *y* line at 11.083 Å. At the temperatures shown, the Na ix satellites *j* and *k* are very weak, the ratio of the sum of these two satellites to the Na x *z* line varying from 0.24 to 0.045 over the range $T_e = 2$ MK to 5 MK. The satellites *q* and *r* are also weak, the feature at 11.15 Å formed by them being unobserved by the FCS. In addition the ratio of blended Na ix *w* to the Ne ix *w4* lines is only weakly T_e -dependent (Figure 3). In fact, the only indication of temperature in the theoretical spectra in Figure 1 is the presence of nearby Fe xvii lines at 11.023 Å, 11.129 Å, and 11.250 Å. The best-fit temperature to the FCS spectrum is clearly $T_e = 3$ MK. However, the emission measure analysis of Landi & Phillips (2005) shows that much of the emission of these and other more highly ionized Fe lines for this particular stage of the August 25 flare occurs at a higher temperature, around $T_e \sim 8$ MK, with He-like ion line emission such as Na x and Ne ix occurring at lower temperatures indicative of the host active region. The agreement of the FCS and theoretical spectra at $T_e = 3$ MK for the Fe xvii lines in Figure 1 may therefore be regarded as coincidental.

As values of temperature over the range 2–5 MK only slightly affect the Na x and Ne ix line emission, the effect of the abundance ratio $A(\text{Na})/A(\text{Ne})$ may be examined; this is shown in Figure 5. The FCS spectrum is compared with theoretical spectra, calculated at $T_e = 3$ MK, for three values of $A(\text{Na})/A(\text{Ne})$: 0.14, 0.07, 0.035, i.e. the coronal value of Feldman et al. (1992a) multiplied by 2, 1, and 0.5 respectively. Clearly the best match is for $A(\text{Na})/A(\text{Ne}) = 0.07$. Ruling out the values of 0.14 and 0.035 for this ratio (top and bottom panels of Figure 5) leads to an estimated precision that is approximately 50%. This estimate of the abundance ratio is significantly larger than the pho-

spheric abundance ratio, $A(\text{Na})/A(\text{Ne}) = 0.02$ (Asplund et al., 2009), and suggests an enhancement of about 3 to 4 in the abundance of Na in the corona if the active region plasma is coronal in origin.

For the Parkinson rocket spectra, the emission arises from a lower-temperature plasma indicative of a non-flaring active region. Figure 2 shows the KAP crystal scans compared with four theoretical spectra with $T_e = 1, 1.5, 2,$ and 2.5 MK and $A(\text{Na})/A(\text{Ne}) = 0.07$. At $T_e \leq 2$ MK, the ratio of the Na x *w*–Ne ix *w4* blend at 11.002 Å to the Na x *z* line at 11.191 Å is sensitive to T_e , largely through the contribution of the Na ix satellites *j* and *k* to Na x line *z*. The ratio of the sum of these satellites to Na x line *z* over the temperature range 1 MK to 2.5 MK varies from 2.5 to 0.14. Of the four theoretical spectra shown, the one with $T_e = 1$ MK best fits the KAP spectrum. Although only just significant (total photon counts per 0.025 s equal to about 16), the feature at 11.15 Å can be identified with the blend of Na ix satellites *q* and *r*; the appearance of these satellites confirms the temperature of ~ 1 MK. This conclusion is also supported by the gypsum crystal scan though this has lower statistical quality. In the original analysis of Parkinson (1975), an emission measure distribution peaking at 3 MK was found, rather more than is found here with improved atomic data. The comparatively low temperature for this active region that we find is in keeping with the fact that solar activity was at a rather low level when the observations were taken.

If the temperature of the active region is only ~ 1 MK, the Fe xvii lines at 11.023 Å, 11.129 Å, and 11.250 Å should not be so strong. The ionization fractions of Bryans et al. (2009) indicate that there is a negligible fraction of Fe^{+16} ions for $T_e \leq 1.5$ MK (Figure 3). As with the FCS spectra, a higher-temperature component might be present. However, in that case the Na x and Ne ix line emission would be much higher, the fitted temperature would be correspondingly higher, and disagreements in the fit to the Na x *w*–Ne ix *w4* blend and the weak 11.15 Å line feature, formed by satellites *q* and *r*, would result. There is a possibility, then, that the Fe^{+16} ion fractions at $T_e \leq 1.5$ MK are in error, and that there is in fact a non-negligible fraction of Fe^{+16} ions at very low temperatures.

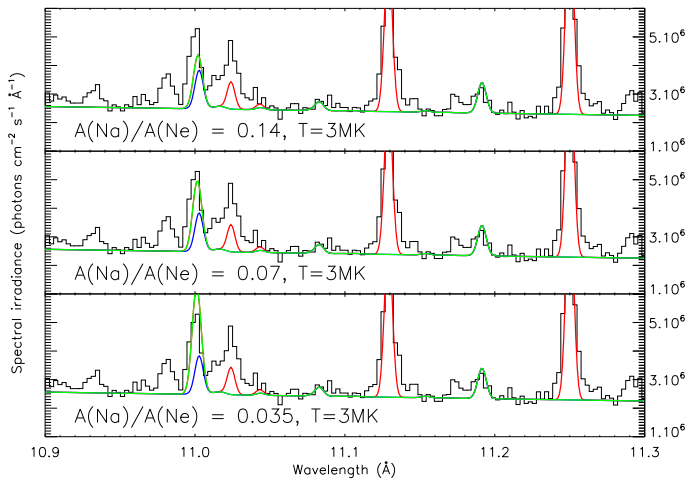


Fig. 5. The FCS spectrum in the 10.9–11.3 Å range during the flare of 1980 August 25 compared with theoretical spectra for $T_e = 3$ MK and three values of the abundance ratio $A(\text{Na})/A(\text{Ne})$ (indicated in each plot). Line styles for the theoretical curves as for Figure 1. Two of the Fe XVII lines are off-scale to show better the agreement of the theoretical curves with the observed Na X and Ne IX line emission. (A colour version is available in the on-line journal. On-line journal version key is the same as for Figure 1.)

5. Conclusions

In this work, recent collisional excitation results for Na X X-ray line emission have been applied to solar spectra for the first time, together with new atomic data for Na IX satellites, formed by both dielectronic recombination and inner-shell excitation. From these and other data from the CHIANTI atomic code, synthetic spectra were calculated as a function of electron temperature T_e . To date, the only observed spectra taken with high-resolution spectrometers in the 10.9–11.3 Å range are from the SMM Flat Crystal Spectrometer (a single scan during the decay of a M1.5 flare) and two rocket-borne scanning crystal spectrometers in 1971 viewing a non-flaring active region. Comparison of the FCS and calculated spectra in the 10.9–11.3 Å range shows that the Na X X-ray lines with nearby Na IX dielectronic satellites yield a Na/Ne abundance ratio through the blend of the Na X w (resonance) line with the Ne IX $w4$ ($1s^2 \ ^1S_0 - 1s4p \ ^1P_1$) line, these lines having almost identical contribution functions $G(T_e)$ for the low temperatures considered here. The value obtained, $A(\text{Na})/A(\text{Ne}) = 0.07 \pm 50\%$, is the coronal value of Feldman et al. (1992a) to within uncertainties. It is significantly higher than the photospheric value, 0.020, and suggests that sodium (like other low-FIP elements) is enhanced by a factor of 3 to 4 in the corona. The lower-temperature observations obtained by Parkinson (1975) are best fitted with theoretical spectra having $T_e = 1$ MK, and are again consistent with a coronal Na/Ne abundance ratio. The presence of Fe XVII lines in these spectra is unexpected, the most recent ionization equilibrium calculations of Bryans et al. (2009) indicating either that there is a higher-temperature component present or (more likely) that there is a negligible fraction of Fe⁺¹⁶ ions at $T_e \leq 1$ MK. A revision of ionization or recombination rates may be needed.

Acknowledgements. K. M. Aggarwal acknowledges financial support from EPSRC. The work of E. Landi is supported by several NASA grants. F. P. Keenan is grateful to AWE Aldermaston for the award of a William Penney Fellowship. We are grateful to Dr Alexander Kramida for help and advice with running the adapted Cowan HFR program. Professor John Parkinson is also thanked for help

and advice on his spectra, as is Dr M. F. Gu for advice on the Flexible Atomic Code used in this work.

References

- Aggarwal, K., Keenan, F. P., & Heeter, R. F. 2009, *Phys. Scripta*, 80, 045301
- Asplund, M., Grevesse, N., Sauval, A. J., & Scott, P. 2009, *Ann. Rev. Astr. Astrophys.* 47, 481
- Bely-Dubau, F., Gabriel, A. H., & Volonté, S. 1979, *MNRAS*, 186, 405
- Bryans, P., Landi, E., & Savin, D. W. 2009, *ApJ*, 691, 1540
- Burkhalter, P. G., Mehlman, G., Apruzese, J. P., Newman, D. A., Scherrer, V. E., Young, F. C., Stephanakis, S. J., & Hinshelwood, D. D. 1990, *J. Quant. Spect. Rad. Trans.*, 44, 495
- Chen, G. X., Smith, R. K., Kirby, K., Brickhouse, N. S., & Wargelin, B. J. 2006, *Phys. Rev. A*, 74, 042709
- Cowan, R. D. 1981, *The Theory of Atomic Structure and Spectra*, University of California Press, Berkeley
- Curdt, W., Landi, E., Wilhelm, K., & Feldman, U. 2000, *Phys. Rev. A*, 62, 022502
- Curdt, W., Brekke, P., Feldman, U., Wilhelm, K., Dwivedi, B. N., Schühle, U., & Lemaire, P. 2001, *A&A*, 375, 591
- Dere, K. P., Landi, E., Mason, H. E., Monsignori Fossi, B. C., & Young, P. R. 1997, *A&AS*, 125, 149
- Dere, K. P., Landi, E., Young, P. R., DelZanna, G., Landini, M., & Mason, H. E. 2009, *A&A*, 498, 915
- Feldman, U., Mandelbaum, P., Seely, J. F., Doschek, G. A., & Gursky, H. 1992, *ApJS*, 81, 387
- Feldman, U. 1992, *Phys. Scripta*, 46, 202
- Feldman, U. 1993, *ApJ*, 411, 896
- Gabriel, A. H. 1972, *MNRAS*, 160, 99
- Gu, M. F. 2003, *ApJ*, 582, 1241
- Hénoux, J. C., & Somov, B. V. 1997, *A&A*, 318, 947
- Landi, E., & Phillips, K. J. H. 2005, *ApJS*, 160, 286
- Meyer, J.-P. 1985, *ApJS*, 57, 173
- Parkinson, J. H. 1975, *Sol. Phys.*, 42, 183
- Phillips, K. J. H., Leibacher, J. W., Wolfson, C. J., Parkinson, J. H., Fawcett, B. C., Kent, B. J., Mason, H. E., Acton, L. W., Culhane, J. L., & Gabriel, A. H. 1982, *ApJ*, 256, 774
- Phillips, K. J. H., Keenan, F. P., Harra, L. K., McCann, S. M., Rachlew-Källne, E., Rice, J. E., & Wilson, M. 1994, *J. Phys. B*, 27, 1939
- Phillips, K. J. H., Chifor, C., & Dennis, B. R. 2006, *ApJ*, 647, 1480
- Phillips, K. J. H., Feldman, U., & Landi, E. 2008, *Ultraviolet and X-ray Spectroscopy of the Solar Atmosphere*, Cambridge University Press (chapter 4)
- Ralchenko, Yu., Kramida, A. E., Reader, J., & the NIST Atomic Spectral Database Team, National Institute of Standards and Technology, Gaithersburg, MD, USA. 2008, Available online at <http://physics.nist.gov/asd3>
- Steenman-Clark, L., Bely-Dubau, F., Faucher, P., Loulergue, M., & Volonté 1984, *Phys. Scr.*, T7, 67
- Sylwester, J., Sylwester, B., & Phillips, K. J. H. 2008, *ApJ*, 681, L117
- Sylwester, J., Sylwester, B., Phillips, K. J. H., & Kuznetsov, V. D., 2010, *ApJ*, 710, 804
- Vainshtein, L. A., & Safronova, U. I. 1978, *Phys. Scripta*, 31, 519
- Walker, A. B. C., Ruge, H. R., & Weiss, H. 1974, *ApJ*, 188, 423
- Wiese, W. L., Smith, M. W., & Miles, B. M. 1969, *Atomic Transition Probabilities*, NSRDS-NBS-22